Comparison of Precipitable Water Observations in the Near Tropics by GPS, Microwave Radiometer, and Radiosondes

YUEI-AN LIOU AND YU-TUN TENG

Center for Space and Remote Sensing Research, and Institute of Space Sciences, National Central University, Chungli, Taiwan

TERESA VAN HOVE

GPS Science and Technology, University Corporation for Atmospheric Research, Boulder, Colorado

JAMES C. LILJEGREN

Environmental Research Division, Argonne National Laboratory, Argonne, Illinois

(Manuscript received 3 January 2000, in final form 26 April 2000)

ABSTRACT

The sensing of precipitable water (PW) using the Global Positioning System (GPS) in the near Tropics is investigated. GPS data acquired from the Central Weather Bureau's Taipei weather station in Banchao (Taipei), Taiwan, and each of nine International GPS Service (IGS) stations were utilized to determine independently the PW at the Taipei site from 18 to 24 March 1998. Baselines between Taipei and the other nine stations range from 676 to 3009 km. The PW determined from GPS observations for the nine baseline cases are compared with measurements by a dual-channel water vapor radiometer (WVR) and radiosondes at the Taipei site. Although previous results from other locations show that the variability in the rms difference between GPS- and WVR-observed PW ranges from 1 to 2 mm, a variability of 2.2 mm is found. The increase is consistent with scaling of the variability with the total water vapor burden (PW). In addition, accurate absolute PW estimates from GPS data for baseline lengths between 1500 and 3000 km were obtained. Previously, 500 and 2000 km have been recommended in the literature as the minimum baseline length needed for accurate absolute PW estimation. An exception occurs when GPS data acquired in Guam, one of the nine IGS stations, were utilized. This result is a possible further indication that the rms difference between GPS- and WVR-measured PW is dependent on the total water vapor burden, because both Taipei and Guam are located in more humid regions than the other stations.

1. Introduction

Precipitable water (PW) plays a crucial role in atmospheric dynamics through the release of huge amounts of latent heat associated with condensation. Knowledge of its distribution is therefore important to better initialize and constrain numerical weather prediction models. Precipitable water is typically measured with radiosonde soundings, which are expensive, both in terms of material cost and labor, and offer limited global coverage. Lidars and Fourier transform infrared spectrometers can profile water vapor, but not above clouds (Solheim et al. 1998). Although solar spectrometers can be used to estimate tropospheric water vapor, the technique is viable only during clear, daytime conditions (Sierk et al. 1997; Plana-Fattori et al. 1998).

Water Vapor Radiometers (WVRs) measure PW and cloud liquid. The method relies on the dominance of water vapor and liquid water in emission and absorption of the atmosphere in the microwave region. For example, measurements at 23.8 and 31.4 GHz with a ground-based radiometer can be used to determine PW and cloud liquid water (Solheim 1993). However, ground-based microwave radiometry is restricted by poor spatial coverage as a result of the relatively high instrument cost, and by its inability to operate during moderate to heavy rain.

A new technique using Global Positioning System (GPS) signals was recently developed to measure PW. Rocken et al. (1993, 1995, 1997) demonstrated ground-based GPS sensing of PW with rms accuracy of 1–2 mm. The retrieved PW data were verified by comparison with WVRs. Businger et al. (1996) summarized the use

Corresponding author address: Dr. Yuei-An Lou, Center for Space and Remote Sensing Research, National Central University, Chungli 320, Taiwan.
E-mail: yueian@csrsr.ncu.tw

of ground-based GPS receivers to retrieve PW. The retrieved PW data were verified by observations of WVR and radiosonde data. Recently, Emardson et al. (1998) reported that differences between WVR and GPS observations of PW are on the order of 1–2 mm based on three-month field measurements in Sweden and Finland. Later, Tregoning et al. (1998) examined the accuracy of absolute PW estimates from GPS observations. They found GPS, radiosonde, and WVR estimates of PW differ by ~1.4 mm between any two kinds of observations with bias ~0.2 mm. They suggested that the most accurate GPS estimates of PW were achieved when the GPS analysis contains station separations of more than 2000 km. Although both Emardson et al. (1998) and Tregoning et al. (1998) demonstrated that PW observed by GPS differs from WVR observations by 1 to 2 mm, their studies were conducted at locations where the atmosphere has a water vapor burden smaller than 2 cm on the average. The accuracy of absolute PW estimated by GPS observations must be reexamined in humid regions where atmospheric water vapor burden is higher and more inhomogeneous.

More recently, Liou et al. (2000) suggested that the agreement of GPS- and WVR-sensed PW scales with the total water vapor burden. Their study was based on GPS measurements from Taipei and Tsukuba, Japan. In this paper, the use of GPS in sensing PW is further investigated by using GPS data acquired in Taiwan and nine IGS stations. Mapping of wet delay onto PW is given in section 2. Descriptions of the field campaign and data processing are summarized in section 3, which also includes specifications of the instruments used in the field campaign. Analysis of the observations is presented in section 4.

2. Mapping of zenith wet delay onto precipitable water

Radio signals transmitted from GPS satellites are delayed by the atmosphere before they are received on the ground. The delay due to the wet component of the troposphere provides the opportunity for sensing water vapor with ground-based GPS. We used GPS data processing software developed by the University of Berne to solve the GPS carrier phase observables for excess optical path length (OPL; Beutler et al. 1996). Zenith wet delay (ΔL_w) was subsequently derived by subtracting zenith hydrostatic delay (ZHD) from the excess OPL, and mapped onto PW by (Bevis et al. 1994)

$$\mathrm{PW} = \Pi \times \Delta L_w, \tag{1}$$

where

$$\Pi = \frac{10^8}{\rho R_v[(k_3/T_m) + k_2']}, \tag{2}$$

and ρ is the density of liquid water (kg m^{-3}), R_v is the specific gas constant of water vapor (461.51 J kg^{-1} K^{-1}), k_2' is 22.1 ± 2.2 (K mb^{-1}), k_3 is (3.739 ± 0.012) × 10^5 (K^2 mb^{-1}), and T_m is the weighted mean temperature of the atmosphere (K),

$$T_m = \frac{\int (P_v/T)\, dz}{\int (P_v/T^2)\, dz}, \tag{3}$$

where P_v is the partial pressure of water vapor (mb), and T is the temperature of the atmosphere (K). In general, Π is about 0.15. However, it is a function of season, location, and weather. Its amplitude may scatter over a range of 20% (Bevis et al. 1994). From 586 radiosonde observations collected at the Taipei site each March from 1988 to 1997, it was found that Π ranges from 0.153 to 0.166, with an average value of 0.159 and a standard deviation of 0.0022.

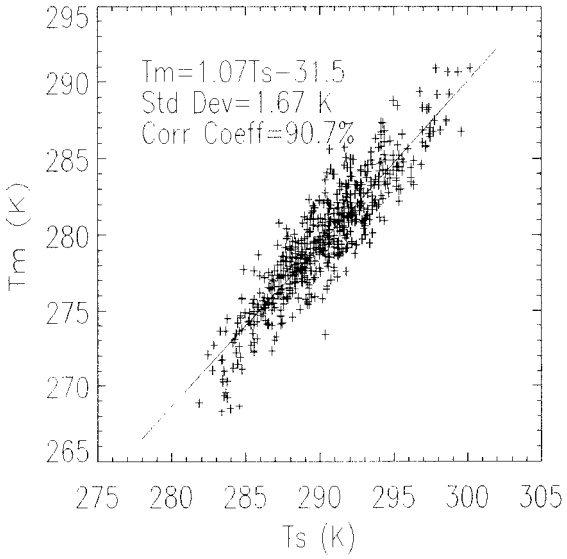

FIG. 1. Weighted mean temperature (T_m) vs surface temperature (T_s) at the Taipei site each Mar from 1988 to 1997.

GPS measurements can be taken as frequently as once per second with the GPS receivers currently deployed in Taiwan. Although there are no available data to provide such high-frequency measurements of the atmospheric profile required for the estimate of T_m, Bevis et al. (1992) suggested that T_m can be estimated by the surface temperature T_s. Figure 1 shows T_m versus T_s observed at the Taipei site each March from the year 1988 to 1997. The correlation coefficient between T_m and T_s reaches as high as 90.7%, which allows the relationship between T_m and T_s to be determined by a least squares fit as

$$T_m = 1.07T_s - 31.5. \tag{4}$$

The root-mean-square (rms) deviation about this regression is 1.67 K. Equation (4) differs from a similar relationship from Bevis et al. (1992), $T_m = 0.72T_s +$

TABLE 1. Ten-year means of T_m observed by radiosondes (raobs) for each month, means of T_m derived by using regression coefficients ($T_m = a\,T_s + b$) from Taipei and Bevis et al. (1992) and the corresponding rmse in T_m between the derived and raobs observed, and the regression coefficients and correlation coefficients (r) between T_m and T_s for the Taipei site.

	Raobs	Taipei regression					Bevis et al. (1992)	
Month	T_m mean	T_m mean	a	b	rmse	r	T_m mean	rmse
Jan	277.49	277.57	1.03	−18.46	1.95	83.7	277.78	2.14
Feb	277.51	275.51	1.04	−21.96	1.67	88.0	277.82	1.91
Mar	279.64	279.60	1.07	−31.51	1.67	90.7	279.16	2.04
Apr	282.49	282.57	0.88	23.33	1.72	88.2	281.76	1.81
May	284.78	284.78	0.83	37.32	1.43	85.1	284.22	1.47
Jun	287.34	287.26	0.83	38.00	1.54	79.7	286.29	1.57
Jul	288.83	288.76	0.83	39.16	1.64	67.9	287.26	1.63
Aug	288.35	288.52	0.93	8.74	1.49	72.8	286.90	1.53
Sep	286.66	286.70	0.99	−3.14	1.34	84.8	285.61	1.45
Oct	284.32	284.04	0.95	2.62	1.36	83.8	283.45	1.45
Nov	281.97	281.97	1.09	−38.14	1.59	89.3	281.45	1.92
Dec	278.88	278.92	0.96	−0.61	1.80	83.9	279.05	1.93

70.2 with a corresponding rms deviation of 4.74 K, using radiosonde data obtained over a two-yr interval from 13 stations in the United States. Table 1 lists 10-yr means of T_m observed by radiosondes for each month, means of T_m derived by using regression coefficients from Taipei and Bevis et al. (1992) and the corresponding root-mean-square error (rmse) in T_m between the derived and radiosonde-observed, and regression coefficients and correlation coefficients between T_m and T_s, for the Taipei site. It is obvious that the use of Taipei regression provides better estimates of T_m. This demonstrates that the relationship between T_m and T_s is site dependent.

To evaluate further the regression (4), we compare the statistics of T_m for the Taipei site in Table 1 with those given by Ross and Rosenfeld (1997) (referred to as RR1997 here for simplicity) who investigated geographic and seasonal variability of T_m based on 23 years of radiosonde soundings at 53 globally distributed stations. It is found that the regression slopes, and correlation between T_m and T_s in this presentation deviate from their corresponding findings in RR1997. Our regression slopes range from 0.83 to 1.09, while theirs range from 0.18 to 0.39 for Guam, 0.43 to 0.79 for Taiyuan of China, and 0.56 to 0.87 for Osan of Korea. Our correlation appears stronger with coefficients of 0.68/0.84 for January/July. In contrast, their correlation is weaker with coefficients of 0.18/0.30 for January/July for Guam, 0.51/0.69 for January/July for Taiyuan of China, and 0.78/0.74 for January/July for Osan of Korea (Fig. 3 of RR1997). These deviations are possibly attributed to the differences in three categories between Taipei and the other three sites: regional weather characteristics, instrumentation uncertainties, and regression treatments. While there are two deviations between two studies, two similarities are observable. First, the correlation between T_m and T_s is weaker in summer and stronger in winter. Second, 11.34 K of annual range of T_m and 283.19 K of annual mean T_m in the current study properly fall onto the corresponding region of the contour plot in Fig. 1 of RR1997. It is found that T_m daily variability is smallest in the Tropics in RR1997. It is of no surprise that our regression differs from that presented of Bevis et al. (1992). Furthermore, we found that the largest rms deviation about the regression for 12 months for the Taipei site is 1.95 K, equivalent to a relative error of 0.70 % (rms deviation/mean), which is smaller than that (slightly larger than 1.0 %) given in Fig. 8 of RR 1997.

Through (2) and (4), T_s can be used to derive Π, which is found to have a mean value of 0.162 with a standard deviation of 0.0021. This approach provides an estimate of Π with a precision of 0.59% and a positive bias of 0.0024, with respect to that derived from radiosondes using (3). We estimated T_m by its linear regression on T_s but T_m appears in the denominator of (2), and thus the relationship between Π and T_m is a nonlinear one. As a result, Π is somehow overestimated when it is derived through the (2)–(4) approach. Hence, a down shifting by 0.0024 is appropriate if one would adopt such an approach to derive Π (denoted by $\hat{\Pi}$). Figure 2 shows the corresponding Π and T_s, which are well correlated with a correlation coefficient of 90.7%. The precision of this approach in deriving Π remains the same if a down shifting is performed. Figure 3 shows the differences between $\hat{\Pi}$ and Π. The differences generally fall onto or near the $\Pi - \hat{\Pi} = 0$ line.

3. Descriptions of field campaign and instruments

To develop and validate the use of GPS in sensing PW, it is required to take concurrent measurements of PW by independent instruments such as WVR and radiosondes. CWB's Taipei weather station is equipped with a GPS dual-frequency receiver, surface meteorological instruments, and radiosondes leaving only the WVR for us to install at the Taipei site from 18 to 24 March 1998. Because the types and accuracy of the instruments are crucial to the determination of the accuracy in sensing PW, all the instruments used in this

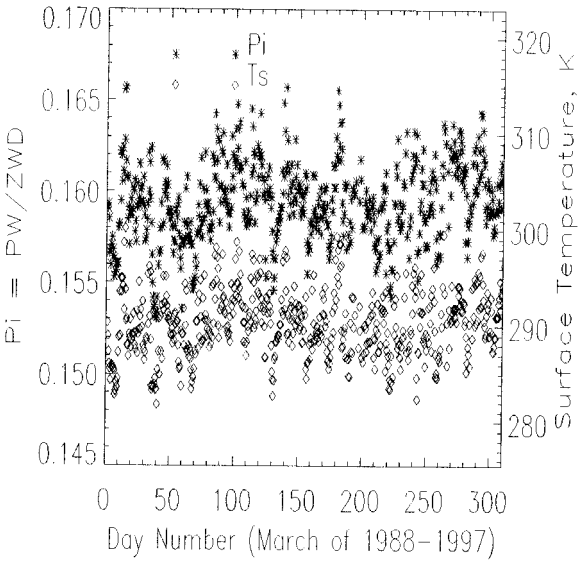

FIG. 2. Π (Pi) derived from radiosonde data and surface temperature at the Taipei site each Mar from 1988 to 1997. PW is precipitable water, ΔL_w is zenith wet delay, and $\Pi = \mathrm{PW}/\Delta L_w$.

study and the data processing means are now summarized.

a. GPS and surface meteorological sensors

Figure 4 shows the geographical locations of the 10 GPS sites from which data are used to obtain ΔL_w and PW at the Taipei site. All the stations with their latitude, longitude, and distances from the Taipei site are listed in Table 2. The antenna types of the GPS instruments

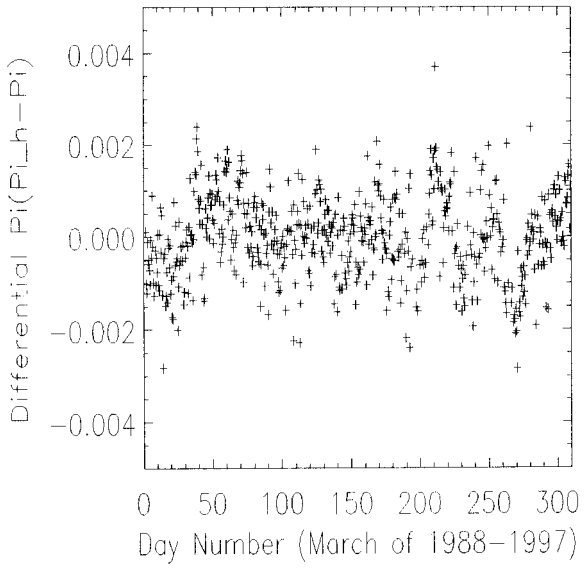

FIG. 3. Difference between Π (=PW/ΔL_w) and $\hat{\Pi}$ at the Taipei site each Mar from 1988 to 1997. Π (Pi) is derived from the radiosondes and $\hat{\Pi}$ (Pi_h) is derived from the surface temperature.

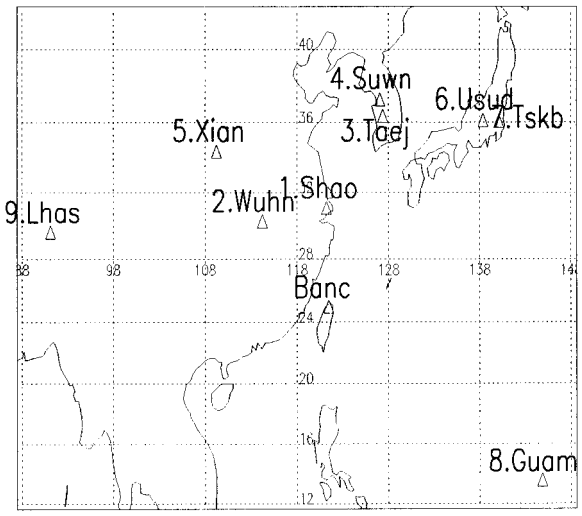

FIG. 4. Geographical locations of the 10 GPS sites, the data for which are used to acquire ΔL_w and PW at the Taipei site.

are Dorne Margolin T except that they are Dorne Margolin B at the Taipei site and TR GEOD L1/L2 GP at the Taejon site. The receiver brands of the GPS instruments are Rogue SNR-8000 except that they are Rogue SNR-8100 at the Sheshan, Lintong, and Tsukuba sites, and Trimble 4000 at the Taejon site. Baselines from Taipei to other nine IGS stations range from 676 to 3009 km so that GPS data acquired from Taipei and any of the other nine stations can be used to derive the absolute excess OPL according to Rocken et al. (1993). Two major steps are performed to determine the baselines. First, the geographical location of the Taipei site is obtained for each day by using the Bernese software provided that a reference IGS station of the Tsukuba site is given a known geographical location. Second, baselines are found by performing fundamental geometric calculations. During the weeklong campaign, GPS data were not available from 1700–0000 UTC on 19 March (GPS time) at the Taipei site, and from 1100–0000 UTC at the Sheshan site for unknown reasons.

TABLE 2. All the stations with their latitude, longitude, and distances from the Taipei site.

Location	Lat (North) (°)	Long (East) (°)	Distance from Taipei (km)
BANC (Taipei, Taiwan)	25.000	121.440	0
1. SHAO (Sheshan, China)	31.100	121.200	676.326
2. WUHN (Wuhan, China)	30.315	114.212	928.157
3. TAEJ (Taejon, Korea)	36.374	127.366	1379.602
4. SUWN (Suwonshi, Korea)	37.276	127.054	1458.713
5. XIAN (Lintong, China)	34.369	109.222	1567.915
6. USUD (Usuda, Japan)	36.133	138.362	2025.541
7. TSKB (Tsukuba, Japan)	36.106	140.087	2155.046
8. GUAM (Dededo, Guam)	13.589	144.868	2739.075
9. LHAS (Lhasa, China)	29.657	91.104	3009.853

TABLE 3. Specifications of the ground-based meteorological sensors used at the Taipei weather station.

Instrument (brand and model)	Measurement range	Accuracy
Pressure (Setra Model 270)	800 to 1100 mb	±0.05% full scale
Temperature (Teledyne Geotech T200)	−50° to 50°C	±0.25°C
Dewpoint (Teledyne Geotech DP-200B)	−30° to 50°C	±1°C

In this study, we analyzed the GPS phase observations using the Bernese GPS software version 4.0 (Beutler et al. 1996). The precise orbits and site positions distributed by the IGS were incorporated into the finding of GPS solutions. The positions of the GPS sites other than the Taipei site were fixed during the week-long campaign. The position of the Taipei site was obtained daily and subsequently fixed, when the data were processed to determine the excess OPL. ZHD was determined by following the surface pressure based formula proposed by Elgered et al. (1991). It simply mimics surface pressure, and, hence, is not shown. Specifications of surface meteorological sensors are given in Table 3. The errors in computing ZHD generated by the pressure sensor are small (<0.35 mm). Figure 5 shows air temperature, dewpoint, precipitation, and relative humidity at the surface. We observe that surface pressure increases from 1011 to 1027 mb from day of year (DoYs) 78 to 80, while surface temperature decreases from 25° to 13°C degrees at the same period of time. This indicates that a cold front followed by high pressure passed over the area. In addition, very little precipitation is seen in the week-long period.

b. Radiosondes

Radiosonde soundings collected at the Taipei site from 18 to 24 March 1998 were used to provide PW.

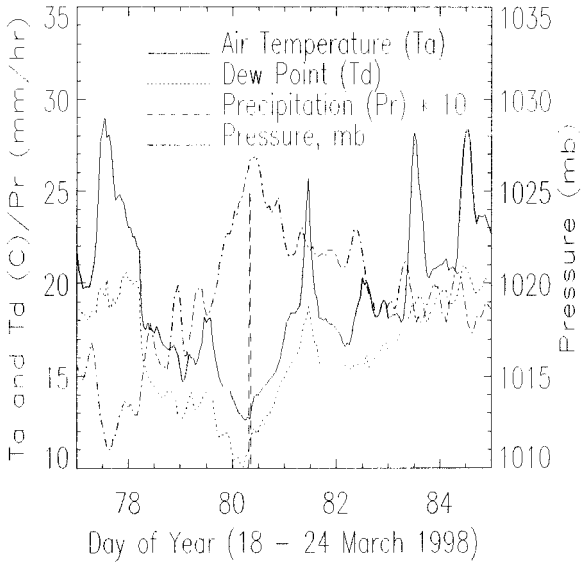

FIG. 5. Air temperature, dewpoint, precipitation, and pressure at the surface at the Taipei site from 18 to 24 Mar 1998.

Specifications of radiosonde are displayed in Table 4. Radiosondes are generally launched twice a day, while only 11 out of 14 launches are valid during the week-long campaign. They measure pressure, temperature, and humidity profiles of the atmosphere. It appears that the errors in PW observed by Vaisala RS2-80MB radiosondes could reach as high as ~6 mm (~4.5 mm by pressure sensor, and ~1.5 mm by humidity sensor). Therefore, PW measured by radiosondes are only used for reference in this paper.

c. Water vapor radiometer

Microwave radiometers measure emissions of the atmosphere that can be used to infer PW and ΔL_w (Westwater 1978). The WVR used in the current study was loaned by Radiometrics Corporation (http://www.radiometrics.
com). Its calibration by a tipping curve method is detailed in Radiometrics (1997). Its specifications are shown in Table 5. The tipping calibration accounts for the different antenna beamwidths for the two operating channels. Clearly, the error caused by the instrumental uncertainty for sensing atmospheric brightness temperature is small, generally 0.3 K. The accuracy of 0.3 K in WVR brightness observations in the two radiometer channels generates a maximum uncertainty of 0.5 mm in PW retrieval, as determined using (5) and the retrieval coefficients given in the caption of Table 6. Han and Westwater (2000) have proposed corrections of radiometer antenna beamwidth, radiometer pointing error, mean radiating temperature error, and horizontal inhomogeneity in the atmosphere on the tipping calibration for ground-based microwave radiometers. These corrections have been found to largely reduce or avoid calibration uncertainties, and hence shall be of great importance for future investigations.

Additional uncertainties are inherent in the WVR data. The WVR observations are not reliable when liq-

TABLE 4. Specifications of the meteorological instruments used at the Taipei weather station.

Instrument (brand and model): radiosonde (RS2-80MB)	Measurement range	Accuracy
Pressure	5 to 1040 mb	±2 mb rms
Temperature	−90° to 50°C	±0.5°C rms
Humidity	1% to 100% RH	±5% RH rms

TABLE 5. Specifications of WVR-1100 loaned by Radiometrics Corp. (Radiometrics 1997).

Operating frequency	23.8/31.4 GHz
Beamwidth	5.7°/4.4°
Sampling rate	User selectable
Accuracy	0.3 K
Resolution	0.25 K
Radiometric range	0 to 700 K
Operating range	−20° to 50°C
Angular coverage	All sky

uid water is present on the radiometer window, or when there is significant scattering from hydrometeors in the field-of-view (Zhang et al. 1999). Furthermore, we notice that additional error could also be produced in the retrieving process. PW and ΔL_w are estimated by a bilinear regression scheme whose coefficients between atmospheric brightnesses at the two operating frequencies and the observables (PW and ΔL_w) are derived using radiosonde soundings collected at the Taipei site each March from the year 1988 to 1997 (Liou 1999). The radiative transfer model developed by the NOAA Wave Propagation Laboratory is used to determine the atmospheric brightness from the radiosonde soundings (Schroeder and Westwater 1991). The model extrapolates the profiles of water vapor, temperature, and pressure to 0.1 mb while determining atmospheric emission, which is dominated by three key constituents of the atmosphere, namely water vapor, liquid water, and oxygen. A comparison of PW derived from WVR observations and radiosonde data is given in Table 6.

The regressions for PW and ΔL_w are

$$\mathrm{PW} = C_{\mathrm{PW0}} + C_{\mathrm{PW1}} \times \mathrm{Tb}_1 + C_{\mathrm{PW2}} \times \mathrm{Tb}_2 \quad \text{and} \quad (5)$$

$$\Delta L_w = C_{\mathrm{ZWD0}} + C_{\mathrm{ZWD1}} \times \mathrm{Tb}_1 + C_{\mathrm{ZWD2}} \times \mathrm{Tb}_2, \quad (6)$$

respectively, where

- C_i are bilinear regression coefficients, where the subscript i represents *PW*0, *PW*1, *PW*2, *ZWD*0, *ZWD*1, and *ZWD*2, and
- Tb_i are observed brightness temperatures of the atmosphere (K), where the subscript $i = 1$ or 2 represents 23.8 and 31.4 GHz, respectively.

4. Results

GPS data acquired at both ends of the nine baseline cases are used to estimate ΔL_w and PW at the Taipei site. The ΔL_w and PW estimates are compared with WVR and radiosonde observations. Because the ratio of ΔL_w to PW is near constant ~6, only PW signatures are shown in the following figures.

a. Comparison in GPS, WVR, and radiosonde observations

Figure 6 shows PW observed by WVR, GPS, and radiosondes at the Taipei site from 18 to 24 March 1998.

TABLE 6. Averages and standard deviations (SD) of PW and ΔL_w observed by radiosonde soundings each Mar from the year 1988 to 1997, and rms differences (rmsd) in PW and ΔL_w between retrievals through (5) and (6) and radiosonde observations. The bilinear regression coefficients are *PW*0 = −0.332, *PW*1 = 0.0975, *PW*2 = −0.0582, *ZWD*0 = −1.469, *ZWD*1 = 0.593, and *ZWD*2 = −0.350.

Atmospheric variable	Average	SD	Retrievals–radiosondes rmsd
PW (cm)	3.65	0.75	0.15
ΔL_w (cm)	22.9	4.59	1.01

GPS solutions from the Taipei–Tsukuba baseline case with a satellite elevation cutoff angle of 12° are chosen as an example. Generally speaking, observations from all of the three techniques match each other reasonably well except for cases where the radiosonde observations appear to be somewhat larger than the other two as listed in Table 7. A best demonstration for the consistency in sensing PW dynamics by GPS and WVR can be illustrated by their observations of a cold front followed by high pressure near DoY = 80 whose obvious decrease in PW from about 4 to 3 cm within 12 h is seen by both GPS and WVR. Since the accuracy of the meteorological sensors onboard radiosonde balloons used by the Taipei site is low and since there are three missing radiosonde soundings during the week of concern, radiosonde observations of ΔL_w and PW are only used for reference without further discussion. While the bias in GPS–WVR observed PW is small (−0.58 mm), the corresponding rms difference is 2.23 mm—larger than the rms accuracy of 1–2 mm reported by others in locations with lower total water vapor burden (Rocken et al. 1995, 1997; Emardson et al. 1998; Tregoning et al. 1998).

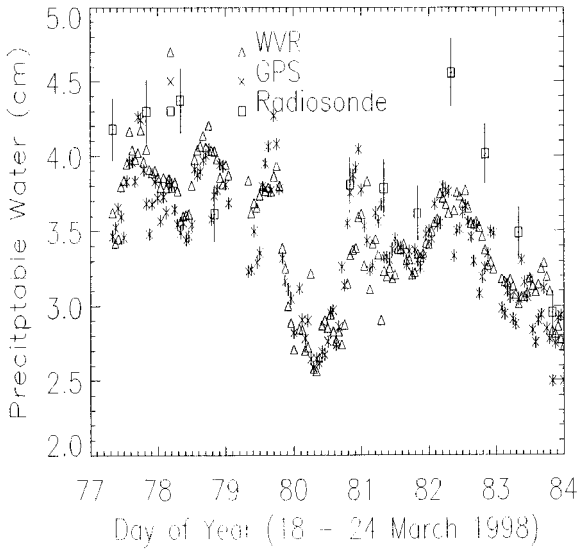

FIG. 6. PW observed by WVR, GPS, and radiosondes at the Taipei site from 18 to 24 Mar 1998. The error bars represent the one-sigma error in radiosonde- and GPS-observed PW.

TABLE 7. Radiosonde, GPS (with a satellite elevation cutoff angle of 12°), and WVR observations of PW and ΔL_w, and rms difference (rmsd) in GPS and WVR observations of PW and ΔL_w at the Taipei site from 18 to 24 Mar 1998, for the Taipei–Tsukuba baseline case.

	Radiosonde		GPS		WVR		GPS–WVR	
Observation	PW	ΔL_w	PW	ΔL_w	PW	ΔL_w	PW	ΔL_w
Average (cm)	3.88	24.1	3.35	21.1	3.41	21.5	−0.058	−0.40
SD or rmsd (cm)	0.46	2.96	0.43	2.64	0.43	2.65	0.223	1.40

Notice that we excluded three GPS outliers and 1 WVR outlier when the rms difference and bias between GPS and WVR measured PW were determined. The three GPS outliers appear to deviate from the nominal values of the PW trend by more than 0.5 cm, while the WVR outlier is abnormally higher than its nominal value of the PW trend by 1.5 cm. This suggests that the agreement between GPS and WVR sensed PW may depend on the total water vapor burden. This possibility should be explored with more extensive comparisons in various humidity regimes.

To demonstrate the scaling effect, we compare PW derived using a Radiometrics WVR-1100 microwave radiometer (Liljegren 1999) operated by the Atmospheric Radiation Measurement (ARM) Program (Stokes and Schwartz 1994) and a GPS receiver near Lamont, Oklahoma, during 1997 (Liljegren et al. 1999). The total number of concurrent GPS and WVR-sensed PW observations is 9085 for the year of 1997. These are divided into six groups corresponding to 0–1, 1–2, 2–3, 3–4, 4–5, or 5–6 cm, respectively, for further analysis. Figure 7 shows (a) variability of GPS–WVR versus GPS-observed PW from the 1997 ARM Program, and (b) the corresponding bias between GPS- and WVR-observed PW. The horizontal axis is determined by using the average of each GPS-sensed PW range. The GPS data were processed using Bernese software. The wet delay estimates are given a 5-mm sigma between the 30-min estimates. This a priori sigma is balanced against the actual GPS data for which a 2-mm sigma is assigned to each 30-s phase measurement from each space vehicle observed. This is not a hard constraint on the amount the wet delay can change at each estimation, but does provide some smoothing. Data down to certain elevation angles of desire were processed. The wet Niell mapping function was used to scale line-of-sight observed delays to zenith for setting up the least squares inversion. Legend notations represent different options for the GPS data processing: dg7w, for 7° minimum angles without ambiguity resolution enabled; dg7wAR, for 7° minimum angles with ambiguity resolution enabled; and dg15w, for 15° minimum angles without ambiguity resolution enabled. The scaling of variability and bias with increased PW can be obviously seen, except in the 3–4 cm range. The rms differences may be small because of editing that excluded cases where there was cloud liquid water detected in the field-of-view of the radiometer, or when there was liquid water on the radiometer window (as indicated by a sensor mounted adjacent to the radiometer window that detects liquid water on its surface). The numbers of WVR data that are rejected by the editing are 1437 for the dg7w case, 1437 for the dg7Arw case, and 1439 for the dg15w case. The numbers of WVR data that pass quality control are in general more than 1000 for the four groups with PW smaller than 4 cm, while they are around 500 for PW = 4–5 cm, and 30 for PW = 5–6 cm. Presence of cloud liquid water in the field-of-view and liquid water on the radiometer window from precipitation or condensation (dew) can increase the uncertainty in determining PW from WVR observations. In addition, comparisons of PW revealed increased bias and variability between the WVR and both the radiosondes and GPS during the summer months that are consistent from year to year and site to site (Liljegren et al. 1999). That is, the larger PW values magnify the error in the comparisons between any two different observing systems.

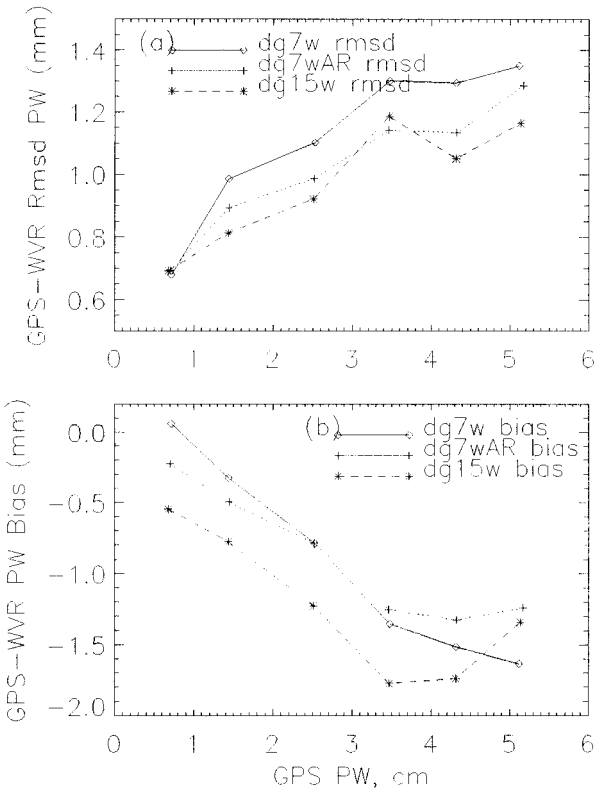

FIG. 7. (a) Variability of GPS–WVR vs GPS-observed PW from the 1997 ARM Program, and (b) the corresponding bias between GPS- and WVR-observed PW.

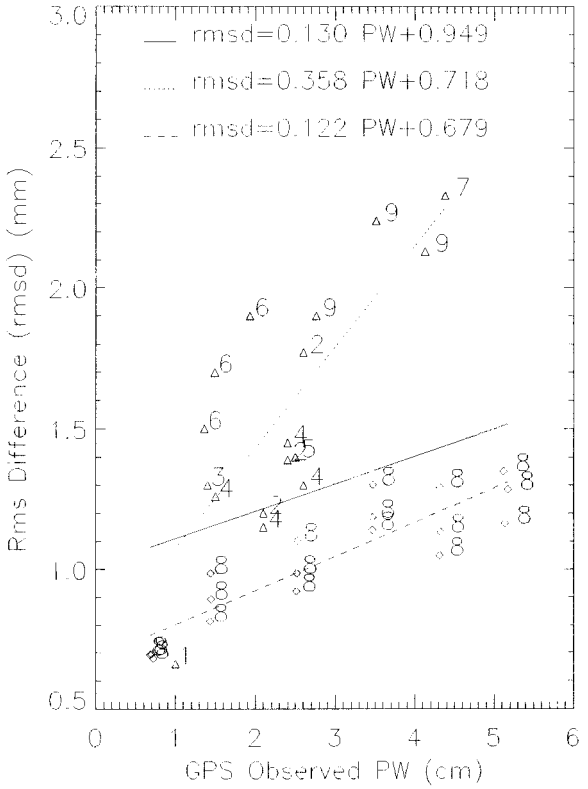

FIG. 8. GPS–WVR-sensed PW variability vs GPS-observed PW reported by various authors, and their best fit to straight lines: dashed line for the 1997 ARM Program data (diamonds—WVR data edited for clear sky conditions only), dotted line for other data (triangles—cloudy conditions included), and solid line for all data.

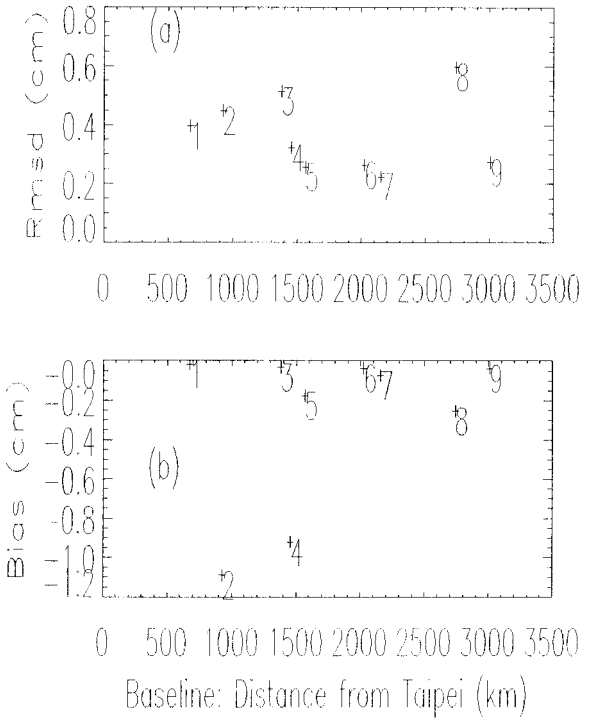

FIG. 9. (a) Rms difference and (b) bias in PW between GPS and WVR observations for the nine baseline cases. Site numbers are given in Table 2.

Figure 8 shows the variability of GPS minus WVR versus GPS-observed PW from various authors: 1) Rocken et al. (1993), PW = ~1.0 cm, rms difference = 0.66 mm (~1.0 cm, 0.66 mm); 2) Rocken et al. (1995), ~2.1 cm, 1.2 mm; ~2.4 cm, 1.39 mm; and ~2.6 cm, 1.77 mm; 3) Rocken et al. (1997), 1.4 cm, 1.3 mm; 4) Duan et al. (1996), 2.1 cm, 1.15 mm; 2.4 cm, 1.45 mm; 2.6 cm, 1.30 mm; and 1.5 cm, 1.26 mm; 5) Tregoning et al. (1998), ~1.5 cm, 1.4 mm; 6) Emardson et al. (1998), 1.93 cm, 1.9 mm; 1.49 cm, 1.7 mm; and 1.36 cm, 1.5 mm; 7) Heymsfield et al. (2000, manuscript submitted to *J. Atmos. Oceanic Technol.*), 4.38 cm, 2.33 mm, 8) Liljegren et al. (1999), (Fig. 7); and 9) current study, 2.76 cm, 1.90 mm (number of WVR and GPS data = 37); 3.51 cm, 2.24 mm (113); and 4.13 cm, 2.13 mm (8) when we performed data analysis similar to the approach for the Lamont case. The numbers followed by the approximation sign "~" indicates that they are determined by an eyeball estimate from the cited papers. The best fits of the variability versus PW to straight lines are indicated by the dashed line for the Lamont data (diamonds), by the dotted line for the other data (triangles), and by the solid line for all data. Notice that all results show the scaling of rms difference with the total water vapor burden. Also, the rms differences are relatively small for the Lamont data because the data were cleaned in a different way by excluding the data for the cases where there was cloud liquid water detected in the field-of-view of the radiometer, or when there was liquid water on the radiometer window. This suggests that the variability depends on the methods used to edit the WVR and GPS data. In addition, we performed an editing upon the Taipei site for a test by using the cases when cloud liquid water is lower than 0.215 mm. The rms difference (corresponding bias) is found to decrease from 2.23 (−0.58) mm for all data to 2.03 (−0.10) mm for the edited data (not included in Fig. 8).

Rocken et al. (1993) suggested that a minimum baseline of 500 km is required to acquire absolute ΔL_w using GPS data, while Tregoning et al. (1998) found that 2000 km is the appropriate minimum requirement. In the following, the impacts of the baseline and, then, satellite elevation cutoff angle on the GPS sensing of PW are examined.

b. Baseline impact on GPS sensing of PW

Figure 9 compares (a) rms difference and (b) bias in PW between GPS and WVR observations for the nine baseline cases. Note that a satellite elevation cutoff angle of 10° is also used in the data processing. The GPS and WVR data were interpolated to provide hourly observations. Rms differences are as large as 4–5 mm with a bias of ~–10 mm when the baselines are smaller than

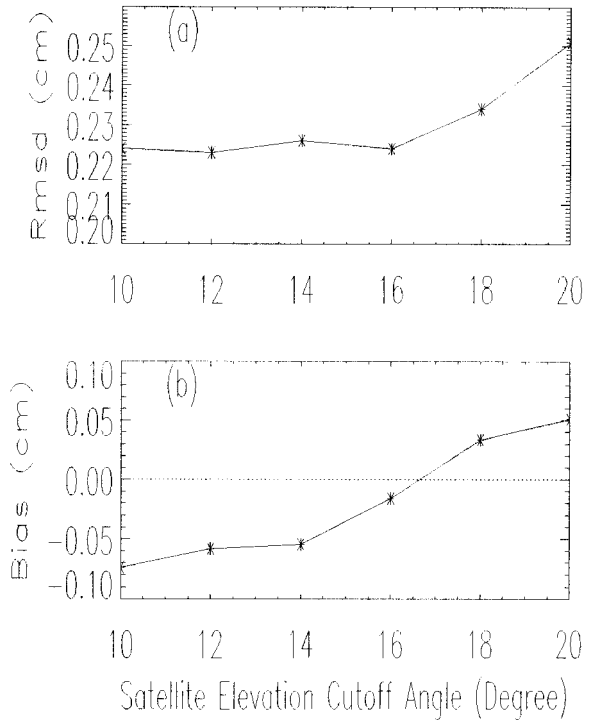

FIG. 10. (a) Rms difference and (b) bias in PW between GPS and WVR observations for six satellite elevation cutoff angles between 10° and 20° in 2° increments for the Taipei–Tsukuba baseline case.

1500 km. The Taipei–Taejon (No. 3) case has high rms difference possibly because of the mixing of antenna types between two sites. Rms differences become smaller ~2.2–2.7 mm with bias <2 mm when the baselines range from 1500 to 3000 km. The exception occurs when GPS data collected at the Guam site (No. 8) were incorporated into the determination of ΔL_w and PW at the Taipei site. For this specific occasion, the rms difference is relatively large ~6.0 mm with bias −2.5 mm. Similar to Taipei, Guam is located in a humid region where the atmosphere is more abundant with water vapor than the other IGS stations. We attribute the increased rms difference to the high total water vapor burden (and its higher variability) at both ends of the baseline.

c. Satellite elevation cutoff angle impact on GPS sensing of PW

Figure 10 shows (a) rms difference and (b) bias in PW between GPS and WVR observations for six satellite elevation cutoff angles between 10° and 20° in 2° increments for the Taipei–Tsukuba baseline case. Extremes of the rms differences in PW occur as minimum 2.23 mm at 12°, and as maximum 2.51 mm at 20°, The biases are small ranging from −0.74 mm at 10° to 0.51 mm at 20°. While both rms differences and biases may vary with cutoff angles, the variations are small. As compared with Fig. 9, GPS solutions are less sensitive to the cutoff angle than the length of baseline within the ranges of our concern.

In section 3, we present instrumental and statistical uncertainties for PW estimations. The maximum values of these uncertainties are about 0.21 mm by the T_s–T_m linear approximation, 0.35 mm by the pressure sensor, 0.5 mm by the WVR approach, and 1.5 mm by the bilinear regression scheme. Since the rms differences in PW between GPS and WVR observations are about 3 mm (much larger than the listed uncertainties of concern), there must exist other uncertainty sources to enlarge the difference between the two instruments. Knowing that the two observing systems measure different volumes of the atmosphere, we suggest that the atmosphere through its inhomogeneity makes a contribution to the enlarged rms difference.

Figure 11 is a diagram of how the GPS, WVR, and radiosonde systems measure different volumes of the atmosphere. Clouds and precipitation are intentionally added into the diagram to produce an inhomogeneous atmosphere that is possibly to increase the difference in ΔL_w and PW observations by the three different observing mechanisms. Such a statement is possibly justified by comparing the observing mechanisms of concern. GPS signals are delayed along the line-of-sight direction, while the computed delays are mapped onto the zenith direction by a stratified atmosphere assumption. WVR-observed brightness temperatures represent an integration of atmospheric emission over a conical volume of the atmosphere. Radiosondes are designed to measure atmospheric profiles along the zenith direction, while they drift with varying wind conditions and require considerable logistics to operate (Leick 1995). That is, there is a great percentage of the time when the three measuring systems of interest observe different volumes of the atmosphere. It is of no surprise, then, that the consistency in ΔL_w and PW estimations by the three observing systems is subject to the degree of atmospheric inhomogeneity. In addition, the calibration of the radiosonde relative humidity sensors may be an important factor in comparison of radiosondes with radiometers and GPS since it may degrade due to the age of radiosonde (Lesht 1997; Liljegren et al. 1997; Westwater et al. 1999). Since Taipei and Guam are located in more humid regions, their atmospheres tend to have more abundant water vapor, and thus water vapor can be more variable and inhomogeneous there than at the other sites considered in this paper. Therefore, variability between radiometer and GPS measurements, with their differences in volumetric sampling of the atmosphere, could increase the variability between GPS- and WVR-observed PW at these sites.

5. Conclusions

GPS observations with surface meteorological measurements can be utilized to derive ΔL_w and PW with high accuracy. We have shown that GPS and a WVR

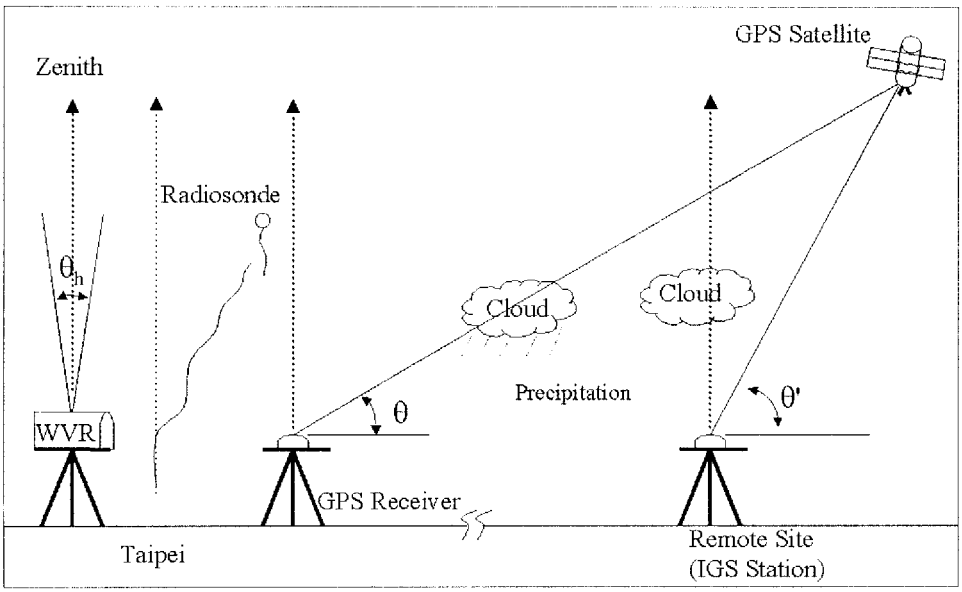

FIG. 11. A diagram showing that the GPS, WVR, and radiosonde estimating systems measure different volumes of the atmosphere. Here, θ and θ' represent the satellite elevation angles at the Taipei and remote sites, respectively. The received GPS signals at angles below the given cutoff angles are not used for our analysis. Here, θ_h is the beamwidth of the dual-channel WVR.

both detect a rapid decrease in PW from about 4 to 3 cm within a 12-h period. While GPS-sensed PW is found to agree with WVR observations with rms accuracy of 1–2 mm in the literature, we found that the best agreement in PW between the two techniques is about 2.2 mm for the nine baseline cases. Furthermore, while we have shown that good agreements with difference in PW by 2.2 mm between the two techniques are achieved for baselines ranging from 1500 to 3000 km, an exception occurs when GPS data acquired from Guam were incorporated into the determination of PW. Both Taipei and Guam are located in humid regions the atmospheres of which are more abundant in water vapor than those in the other IGS stations of our interest. This possibly indicates that the difference between GPS and WVR PW estimates scales with the total water vapor burden. By comparing the variability of GPS minus WVR versus GPS-observed PW from various studies in the literature, we found that the variability also depends on the methods used to edit the WVR and GPS data. In addition, we have shown that the agreement between GPS and WVR PW estimates is less sensitive to satellite cutoff angle than the length of the baseline.

Acknowledgments. This work was supported in part by grants from NSC87-2621-P-008-016 for GPS data processing, NSC87-NSPO(A)-PC-FA07-06 for the WVR experiment, and Center for Space and Remote Sensing Research. James Liljegren was supported by the Environmental Sciences Division of the U.S. Department of Energy as part of the Atmospheric Radiation Measurement Program under Contracts CHENG82-1010502-0002884 at Ames Laboratory and W-31-109-Eng-38 at Argonne National Laboratory. The authors thank Radiometrics Corporation for the loan of a WVR, CWB for providing GPS data from the Taipei site and a space to conduct the WVR experiment, NOAA Forecast Systems Lab for providing GPS data from the Lamont site, and Dr. R. Ware for technical advice. The authors also thank Dr. Ed R. Westwater and two anonymous reviewers for their useful comments about the original manuscript.

REFERENCES

Beutler, G., and Coauthors, 1996: *Bernese GPS Software Version 4.0.* University of Berne, 418 pp.

Bevis, M., S. Businger, T. A. Herring, C. Rocken, R. A. Anthes, and R. H. Ware, 1992: GPS meteorology: Remote sensing of atmospheric water vapor using the Global Positioning System. *J. Geophys. Res.*, **97,** 15 784–15 801.

——, ——, S. Chiswell, T. A. Herring, R. A. Anthes, C. Rocken, and R. H. Ware, 1994: GPS meteorology: Mapping zenith wet delays onto precipitable water. *J. Appl. Meteor.*, **33,** 379–386.

Businger, S., and Coauthors, 1996: The promise of GPS in atmospheric monitoring. *Bull. Amer. Meteor. Soc.*, **77,** 5–18.

Duan, J., and Coauthors, 1996: GPS meteorology: Direct estimation of the absolute value of precipitable water. *J. Appl. Meteor.*, **35,** 830–838.

Elgered, G., J. L. Davis, T. A. Herring, and I. I. Shapiro, 1991: Geodesy by radio interferometry: Water vapor radiometry for estimation of the wet delay. *J. Geophys. Res.*, **96,** 6541–6555.

Emardson, T. R., G. Elgered, and J. Johansson, 1998: Three months of continuous monitoring of atmospheric water vapor with a network of GPS receivers. *J. Geophys. Res.*, **103,** 1807–1820.

Han, Y., and E. R. Westwater, 2000: Analysis and improvement of tipping calibration for ground-based microwave radiometers. *IEEE Trans. Geosci. Remote Sens.*, **38**, 1260–1276.

Leick, A., 1995: *GPS Satellite Surveying.* John Wiley and Sons, 560 pp.

Lesht, B., 1997: An internal analysis of SGP/CART radiosonde performance during WVIPO-96. *Sixth Atmospheric Radiation Measurement Program Science Team Meeting,* San Antonio, TX, U.S. Department of Energy, 59–62.

Liljegren, J., 1999: Automatic self-calibration of ARM microwave radiometers. *Microwave Radiometry and Remote Sensing of the Earth's Surface and Atmosphere,* P. Pampaloni and S. Paloscia, Eds., VSP, 552 pp.

——, B. Lesht, E. Westwater, and Y. Han, 1997: A comparison of integrated water vapor sensors: WVIOP-96. *Sixth Atmospheric Radiation Measurement Program Science Team Meeting,* San Antonio, TX, U.S. Department of Energy, 1–4.

——, ——, T. Van Hove, and C. Rocken, 1999: A comparison of integrated water vapor from microwave radiometer, balloon-borne sounding system and Global Positioning System. *Ninth Atmospheric Radiation Measurement Program Science Team Meeting,* San Antonio, TX, U.S. Department of Energy, 1–8.

Liou, Y.-A., 1999: Ground-based radiometric sensing of atmospheric dynamics in precipitable water vapor. *Atmos. Sci.,* **27,** 141–158.

——, C.-Y. Huang, and Y.-T. Teng, 2000: Precipitable water observed by ground-based GPS receivers and microwave radiometry. *Earth Planets Space,* **52**, 445–450.

Plana-Fattori, A., M. Legrand, D. Tanre, C. Devaux, and A. Vermeulen, 1998: Estimating the atmospheric water vapor content from sun photometer measurements. *J. Appl. Meteor.,* **37,** 790–804.

Radiometrics, 1997: WVR-1100 Water Vapor and Liquid Water Radiometer. Radiometrics Corporation, 30 pp. [Available from Radiometrics Corporation, 2840 Wilderness Place, Unit G, Boulder, CO 80301-5414.]

Rocken, C., R. Ware, T. Van Hove, F. Solheim, C. Alber, J. Johnson, M. Bevis, and S. Businger, 1993: Sensing atmospheric water vapor with the Global Positioning System. *Geophys. Res. Lett.,* **20,** 2631–2634.

——, T. Van Hove, J. Johnson, F. Solheim, R. Ware, M. Bevis, S. Businger, and S. Chiswell, 1995: GPS/STORM—GPS sensing of atmospheric water vapor for meteorology. *J. Atmos. Oceanic Technol.,* **12,** 468–478.

——, ——, and R. Ware, 1997: Near real-time GPS sensing of atmospheric water vapor. *Geophys. Res. Lett.,* **24,** 3221–3224.

Ross, R. J., and S. Rosenfeld, 1997: Estimating mean weighted temperature of the atmosphere for Global Positioning System applications. *J. Geophys. Res.,* **102,** 21 719–21 730.

Schroeder, J. A., and E. R. Westwater, 1991: Users' guide to WPL microwave radiative transfer software. NOAA Tech. Memo. ERL WPL-213, 84 pp.

Sierk, B., B. Burki, H. Becker-Ross, S. Florek, R. Neubert, L. P. Kruse, and H. Kahle, 1997: Tropospheric water vapor derived from solar spectrometer, radiometer, and GPS measurements. *J. Geophys. Res.,* **102,** 22 411–22 424.

Solheim, F., 1993: Use of pointed water vapor radiometer observations to improve vertical GPS surveying accuracy. Ph.D. dissertation, University of Colorado, 128 pp. [Available from Radiometrics Corporation, 2840 Wilderness Place, Unit G, Boulder, CO 80301-5414.]

——, J. R. Godwin, E. R. Westwater, Y. Han, S. J. Keihm, K. Marsh, and R. Ware, 1998: Radiometric profiling of temperature, water vapor and cloud liquid water using various inversion methods. *Radio Sci.,* **33,** 393–404.

Stokes, G. M., and S. E. Schwartz, 1994: The Atmospheric Radiation Measurement (ARM) Program: Programmatic background and design of the Cloud and Radiation Testbed. *Bull. Amer. Meteor. Soc.,* **75,** 1201–1221.

Tregoning, P., R. Boers, D. O'Brien, and M. Hendy, 1998: Accuracy of absolute precipitable water vapor estimates from GPS observations. *J. Geophys. Res.,* **103,** 28 701–28 710.

Westwater, E. R., 1978: The accuracy of water vapor and cloud liquid determinations by dual-frequency ground-based microwave radiometry. *Radio Sci.,* **13,** 677–685.

——, and Coauthors, 1999: Ground-based remote sensor observations during PROBE in the tropical western Pacific. *Bull. Amer. Meteor. Soc.,* **80,** 257–270.

Zhang, G., J. Vivekanandan, and M. K. Politovich, 1999: Scattering effects on microwave passive remote sensing of cloud parameters. Preprints, *Eighth Conf. on Aviation, Range, and Aerospace Meteorology,* Dallas, TX, Amer. Meteor. Soc., 497–501.